Journal of Athletic Training 2025;60(6):414–428
doi: 10.4085/1062-6050-0698.23

www.natajournals.org

Chronic Ankle Instability–Related Outcomes Associate With Ankle-Joint Loading During Walking

Jaeho Jang, PhD, ATC*; J. Troy Blackburn, PhD, ATC†; Joshua N. Tennant, MD‡; Jason R. Franz, PhD§; Brian G. Pietrosimone, PhD, ATC†; Erik A. Wikstrom, PhD, ATC†

*Department of Kinesiology, University of Texas at El Paso; †MOTION Science Institute, Department of Exercise and Sport Science; ‡Department of Orthopaedics, University of North Carolina at Chapel Hill; §Joint Department of Biomedical Engineering, University of North Carolina at Chapel Hill and North Carolina State University, Chapel Hill

Context: Recurrent trauma and altered biomechanics in those with chronic ankle instability (CAI) have been linked to altered joint loading. Previous studies revealed that patients with CAI exhibit altered joint contact force (JCF) profiles relative to uninjured individuals during walking and landing. Identifying more easily obtainable outcomes that are associated with ankle JCF in those with CAI would reduce the knowledge gap between loading profiles at the ankle joint and outcomes related to CAI.

Objective: To quantify how ankle JCF, structural measures, postural control, and walking biomechanics interrelate in patients with CAI and how CAI variables predict ankle JCF.

Design: Cross-sectional study.

Setting: Research laboratory.

Patients or Other Participants: A total of 21 patients with CAI (7 men, 15 women; age = 23 ± 4 years, height = 171.6 ± 8.3 cm, mass = 71.7 ± 12.1 kg).

Main Outcome Measure(s): Triaxial peaks, impulses, and loading rates of ankle JCF were captured. Rearfoot alignment, Star Excursion Balance Test reach distances, weight-bearing lunge test score, and peak ankle angles and moments during the stance phase of walking were also recorded. Partial Pearson *r* correlations and forward stepwise regressions were used to examine the relationships among the ankle JCF variables and traditional CAI-related impairments.

Results: Less compressive JCF variables were associated with more rearfoot varus alignment ($r = -0.53$, $P = .02$) and greater peak inversion moment while walking ($r = -0.46$, $P = .041$). Greater posterior JCF was associated with greater peak eversion ($r = 0.55$, $P = .01$) and dorsiflexion moments while walking ($r = -0.48$, $P = .03$) as well as less rearfoot varus alignment ($r = 0.51$, $P = .02$). Similarly, greater lateral JCF variables were associated with greater dorsiflexion moment while walking ($r = 0.49$, $P = .03$) as well as less rearfoot varus alignment ($r = -0.52$, $P = .02$). Multivariate regression models partially explained ankle JCF while walking in those with CAI.

Conclusions: Although our results suggest potential associations between gait biomechanics, structural measures, and postural control with ankle JCF, further research is needed to determine if targeting these factors during therapeutic interventions would modify mechanical loading at the ankle joint during walking.

Key Words: joint contact force, musculoskeletal modeling, OpenSim

Key Points

- Greater rearfoot varus alignment and peak inversion moment at push-off were associated with less compressive ankle joint contact force (JCF).
- Greater peak eversion and dorsiflexion moment at heel strike were associated with greater posterolateral ankle JCF.
- Less rearfoot varus alignment was associated with greater posterolateral ankle JCF.

Lateral ankle sprains are common musculoskeletal injuries in sports and activities of daily living, and up to 40% of these sprains result in chronic ankle instability (CAI).[1] Patients with CAI commonly have various symptoms such as pain, swelling, loss of function, repetitive lateral ankle sprains, and a sensation of "giving way."[2] As a result, patients with CAI develop altered movement strategies to compensate for their specific set of impairments (ie, neuromuscular, structural, or both).[3] These maladaptive movement patterns result in an increased risk of recurrent lateral ankle sprains and altered biomechanics across various activities including walking.[2,3] Similarly to other musculoskeletal injuries such as anterior cruciate ligament rupture, recurrent trauma and altered biomechanics in individuals with CAI have been linked to altered cartilage loading.[4] Altered cartilage loading has been hypothesized to be a potential contributor to the early onset of ankle-joint degeneration and subsequent posttraumatic osteoarthritis, but further research is needed to establish a definitive causal link.[5,6]

Altered walking biomechanics (ie, kinematic, kinetic, and spatiotemporal variables) in patients with CAI have been associated with deleterious biochemical changes within the talar joint, subtalar joint, or both.[7] Biochemical alterations within cartilage have also been linked to joint degeneration.[8] Despite these associations, kinetic variables such as ground reaction force (GRF) and joint moments are oversimplified, as the contributions of muscle forces, the biggest contributor to joint loading, are not considered.[9] Joint loading is the sum of external forces (ie, GRF), muscle forces, and passive ligamentous forces (ie, capsuloligamentous stability) and is quantified via joint contact force (JCF).[10] Traditional kinetic and kinematic variables represent only a fraction of the factors of joint loading because muscle contributions are not accounted for. This suggests that those traditional biomechanical variables might not be robust enough for the study of joint loading; thus, JCF needs to be obtained to further study the effect of joint loading in those with CAI. By using musculoskeletal modeling, we can quantify JCF based on indirectly calculated individual muscle forces using typical kinematic (ie, 3-dimensional motion capture) and kinetic (ie, GRF) data.[10] During the stance phase of walking, individuals with CAI exhibit lower compressive JCF at heel strike but greater posterior and lateral shear JCF at push-off compared with uninjured controls.[11]

To date, no nonoperative treatments are available to slow the early onset of ankle-joint degeneration due to CAI[5] despite evidence that early interventions targeting modifiable factors to prevent disease progression are required.[6] Although quantifying JCF in patients with CAI provides a more nuanced examination of the mechanical joint loading at the ankle, it does not, in isolation, advance our ability to develop or deploy interventions that could potentially slow the degenerative process. In addition, quantifying JCF requires specialized equipment, training, and computational time. Identifying more easily obtainable outcomes that are associated with ankle JCF in those with CAI would reduce the existing knowledge gap regarding the association between CAI-related outcomes and altered ankle-loading profiles in patients with CAI and help drive future investigations that facilitate the clinical application of such information. For example, structural changes (eg, rearfoot varus), poor postural control, and altered walking biomechanics (eg, laterally deviated foot position) observed in those with CAI are modifiable and linked to markers of compositional change in ankle cartilage, but future research is needed to determine if modifying such outcomes via therapeutic interventions positively affects cartilage composition.[7]

The purpose of our preliminary study was 2-fold: (1) to quantify associations among ankle JCF variables and structural measures, postural control, and walking biomechanics in patients with CAI and (2) to examine how combinations of CAI-related variables predict triaxial ankle JCF in those with CAI via multivariate regression models. Based on previous research and unpublished research from our laboratory, we hypothesized that lower compressive JCF would be associated with smaller peak plantar-flexion moment and worse weight-bearing lunge test (WBLT) and Star Excursion Balance Test (SEBT) scores but greater peak inversion moment and rearfoot varus.[7,11,12] We also hypothesized that greater posterior and lateral JCF would be associated with greater peak eversion moment and rearfoot varus but smaller peak dorsiflexion angle and lower WBLT and SEBT scores. Finally, we hypothesized that ankle JCF could be predicted via combinations of CAI biomechanical impairments.

METHODS

Participants

The data reported herein are from a larger study that was powered to investigate differences in ankle JCF and muscle-force contributions to ankle JCF during walking across patients with CAI, uninjured control, and copers. Thus, we used our maximum available sample size of 21 patients with CAI (7 men, 15 women; age $= 23 \pm 4$ years [range, 18–45 years], height $= 171.6 \pm 8.3$ cm, mass $= 71.7 \pm 12.1$ kg) to address our research questions. Based on the selection criteria of the International Ankle Consortium, we recruited patients with CAI only if they had a history of $\geq$1 lateral ankle sprain, $\geq$2 episodes of giving way within 6 months, Identification of Functional Ankle Instability (IdFAI) score of $>$11, Foot and Ankle Ability Measure (FAAM)–Activities of Daily Living score of $<$90%, and FAAM-Sports score of $<$80%.[13] Three participants had bilateral CAI. We selected the limb with the greater (worse) IdFAI score for these 3 participants. Based on the recommended exclusion criteria of the International Ankle Consortium, we excluded individuals who had acute lower extremity or head injuries within 3 months before the study, chronic musculoskeletal injuries to their lower extremity (eg, tear of a major ligament), vestibular and visual issues, or a history of any lower extremity surgery. The study was approved by the Institutional Review Board of the University of North Carolina at Chapel Hill, and all participants provided written informed consent.

Procedures

We measured participants' self-selected walking speed during 5 overground walking trials within a 6-m walkway using infrared timing gates (Dashr 2.0; Dashr Motion Performance Systems). Next, we placed a total of 41 retroreflective markers bilaterally on the first toes, first and fifth metatarsals, lateral and medial malleoli, peroneal tuberosities, sustentaculum tali, calcanei, shanks (4-marker clusters), medial and lateral femoral epicondyles, midthighs, greater trochanters, anterior-superior (AP) iliac spines, posterior-superior iliac spines, and acromion processes. In addition, markers were placed on the sacrum, intervertebral space between L4 and L5, and sternum. An 8-camera motion-capture system (Qualisys Miqus) was used for 3-dimensional motion capture during walking on the Bertec Fully Instrumented Treadmill (Bertec Corp), a split-belt instrumented treadmill. The coordinate system of our laboratory was aligned with the standard engineering system for OpenSim (version 4.0; Stanford University) analyses, where X is forward, Y is up, and Z is right. Angles represent proximal to distal segment motion, and all moments are internal: plantar-flexion is negative, dorsiflexion is positive, inversion angles and moments are positive, and eversion is negative. Kinematic and kinetic data were sampled at 200 and 2000 Hz, respectively. When participants were prepared, we captured a static calibration trial. All participants had a familiarization trial on the treadmill at their self-selected speed for up to 5 minutes. Next, we recorded their walking biomechanics on the treadmill at their self-selected speed for 2 minutes. Postcollection, we processed marker trajectories and GRF data using a fourth-order Butterworth filter with a cutoff frequency of 12 Hz in MATLAB (version R2022b; MathWorks). We analyzed a total of 50 stance phases of walking during the second minute of data collection after screening for the maximum number of available stances that did not cross the midline of the treadmill. The *stance phase* of walking was defined as the interval from ipsilateral heel strike (ie, GRF $>$ 20 N) to toe-off (ie, GRF $<$ 20 N) of the involved limb. Any steps that crossed the midline of the instrumented treadmill were replaced with the ones that did not cross the midline.

Data Acquisition and Analysis

Joint Contact Force. To calculate ankle JCF, we deployed a validated full-body musculoskeletal model (ie, Rajagopal et al, OpenSim 4.0) with 37 degrees of freedom and 80 Hill-type muscle-tendon units for the lower extremity.[14] This widely used model, specifically designed to study human gait, was selected because of its validation during walking and its use of anatomic data from cadavers and magnetic resonance images of healthy individuals.[14] Specifically, on release, the model was validated for walking and running by comparing its inverse dynamics with muscle-generated joint moments from simulations and checking computed muscle activations against electromyography for major lower body muscles during these activities. Participants' models were scaled to their anthropometric data using a static calibration trial. We also updated the maximum isometric forces (*MaxIso*) of all muscles via generic (*C*) and participant-specific (*S*) multipliers using participants' estimated lower extremity muscle volume, which was derived from mass (*m*) and height (*h*) (Equations 1–3).[15] The main goal of this approach was to incorporate participant-specific anthropometric factors into a generic model. Without additional processes, the maximum isometric force that a model can generate will not be appropriately scaled; rather, it will be the same for all participants.

$$F_{Subject}^{MaxIso} = F_{Generic}^{MaxIso} \times (C \times S) \tag{1}$$

$$S = \frac{MuscleVolume_{Subject}}{MuscleVolume_{Model}} \tag{2}$$

$$Muscle\ Volume = 47mh + 1285 \tag{3}$$

The inverse kinematics and inverse dynamics pipelines were used to determine joint kinematics and moments in the sagittal and frontal planes during the stance phase of walking. Kinematic variables included peak plantar-flexion, dorsiflexion, inversion, and eversion angles. Kinetic variables included peak plantar-flexion, dorsiflexion, inversion, and eversion moments during the stance phase of walking, scaled to body weight (Figure 1). The residual reduction algorithm used inverse kinematics and GRF data to update model parameters iteratively by using a recently published automated algorithm in MATLAB until residual forces and moments become smaller than "*good*" threshold values according to OpenSim user's guidelines.[16] The static optimization pipeline was used to resolve net joint moments into individual muscle forces by minimizing the sum of muscle activations to the exponent of 3, and the analysis tool was used to estimate triaxial ankle JCFs (compressive, AP, and medial-lateral) during walking stance.[17]

We assessed ankle JCF using the following 3 key variables: peak (highest value), impulse (area under the curve, indicating total mechanical loading), and loading rate (LR; speed of mechanical loading).[11] Our analysis of the 3 JCF variables was guided by a previous study in which researchers explored the differences in medial knee JCF between individuals with and without limb loss because these variables could serve as indicators of ankle JCF patterns during walking in those with CAI—a subject that, to our knowledge, remains largely unexplored.[18] For AP and mediolateral shear JCF, we divided the curve into 2 and 3 phases, respectively, based on the moment(s) the curve crossed zero. We defined the peak, impulse, and LR in each phase. Positive vectors in AP and mediolateral JCF represented anterior and lateral directions, and negative vectors indicated posterior and medial directions (Figure 2). Our chosen JCF variables were based on differences observed between those with and without CAI in a previous study and unpublished research from our laboratory.[11]

Rearfoot Alignment. We measured rearfoot alignment during WB (standing) and non–WB (NWB; prone).[19,20] The intraclass correlation coefficients for intrarater and interrater reliability for the rearfoot measure were 0.87 and 0.85, respectively.[20] We took a digital photograph (Galaxy Tab S2 9.7″; Samsung) of the posterior aspect of the leg. Using publicly available image processing software (ImageJ; National Institutes of Health), we measured rearfoot alignment as the angle between lines that bisected the leg and the calcaneus (Figure 3). The leg was bisected by drawing a line between the midpoint of the widest point of the calf and the midpoint between the malleoli. This line was intersected by the calcaneal line, which was drawn from the center of the heel to the midpoint between the malleoli. For each angle, 3 measurements were taken, and the average of those measurements were used in the final analyses.

Dorsiflexion Range of Motion. We used the WBLT to measure dorsiflexion range of motion by averaging the scores from 3 trials.[21] Participants were allowed to support themselves against a wall for balance while the heel remained in contact with the floor. They were allowed to rest their nontest limb behind the test limb in a comfortable position. We measured the maximum distance from the big toe to the wall (in centimeters) as long as the test knee touched the wall and the heel stayed in contact with the ground. The following oral instructions were given to participants: "Touch the wall with your kneecap by lunging forward while keeping your heel on the ground."

Dynamic Postural Control. We used the modified SEBT to measure dynamic postural control of the involved limb by averaging 3 trials of 3 reach directions: anterior, posteromedial (SEBT-PM), and posterolateral.[22] Participants placed the tip of the big toe in the grid center for the anterior direction and the heel at the grid center for the 2 posterior directions. Both hands were placed on the hips during testing. Participants reached as far as possible in the 3 reach directions with the unaffected limb. At least 4 practice trials in each direction were allowed for familiarization with the task before beginning the testing protocol. Only trials in which participants could touch the ground during their reach without accepting weight and maintaining balance through the return to their original position were used for the final analysis. All distances were scaled to participants' *leg length*, which was defined as the distance from the AP iliac spine to the ipsilateral medial malleolus.

Statistical Analysis

The primary independent variables were biomechanical: ankle-joint sagittal- and frontal-plane angles and moments at the first and second peaks during the stance phase of walking. The secondary independent variables were WBLT and SEBT. We measured the strength of a linear relationship between the JCF variables and the independent variables by examining pairwise correlations. We calculated the partial Pearson *r* correlation, correcting for participants' gait speed

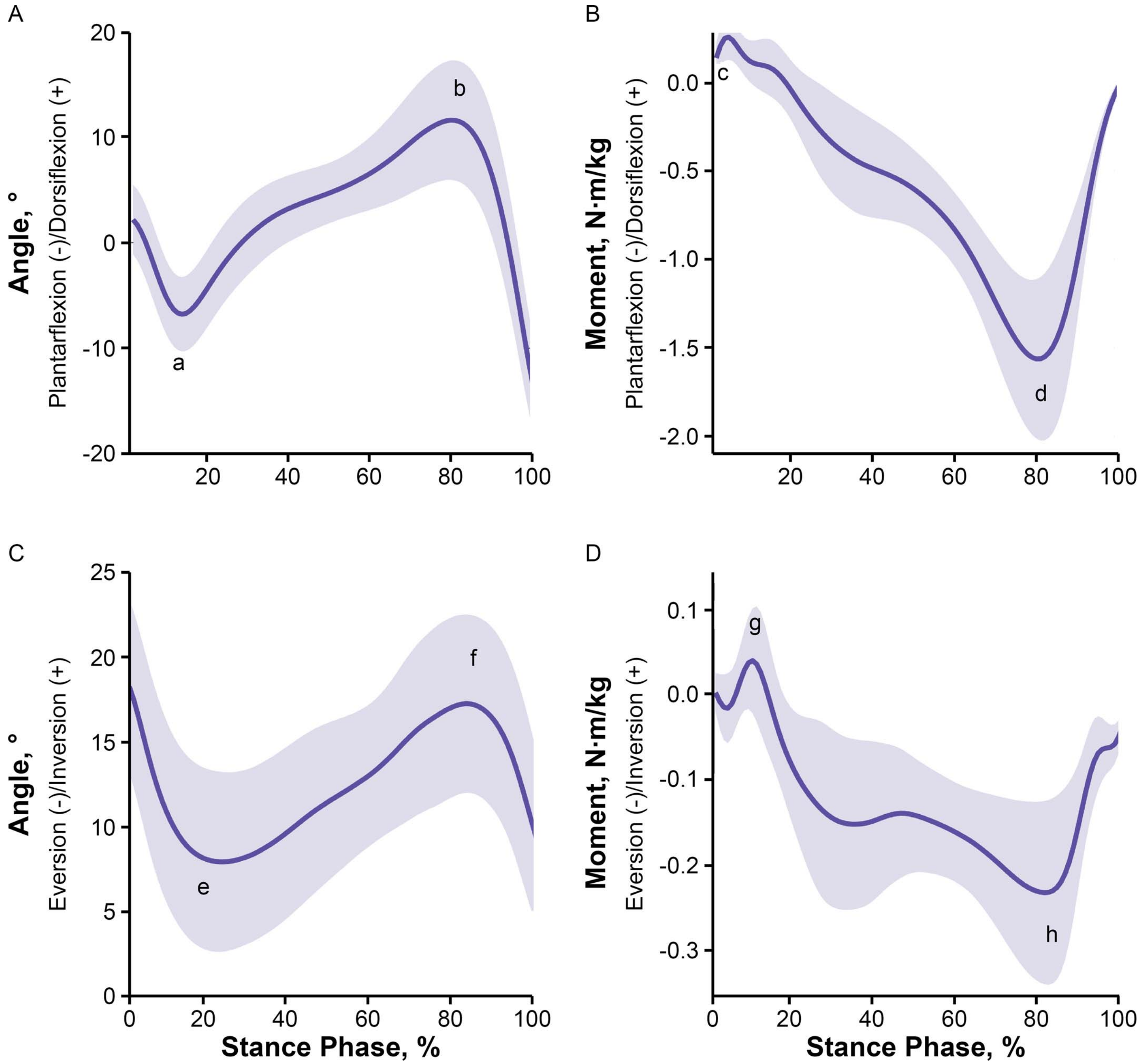

Figure 1. Ankle excursion and moment in the sagittal and frontal planes during the stance phase of walking. A, Sagittal-plane ankle excursion. B, Sagittal-plane ankle moment. C, Frontal-plane ankle excursion. D, Frontal-plane ankle moment. [a] Peak plantar-flexion angle. [b] Peak dorsiflexion angle. [c] Peak dorsiflexion moment. [d] Peak plantar-flexion moment. [e] Peak eversion angle. [f] Peak inversion angle. [g] Peak inversion moment. [h] Peak eversion moment.

because gait speed influences ankle kinematics and kinetics. In this context, coefficients of 1 and -1 represent perfect positive and negative correlation, respectively, and 0 represents no linear relationship. Correlations of $0.1 \leq r < 0.3$ were interpreted as *small*; $0.3 \leq r < 0.5$, *moderate*; and $r \geq 0.5$, *large*. Next, we conducted forward stepwise selection multivariable linear regressions if multiple predictors ($k \geq 2$) with r values of $\geq$0.3 were present, where k represents the number of qualifying independent variables. This approach aimed to identify combinations of variables that best explained the JCF peak, impulse, and LR in triaxial directions. We set the α level a priori at .05 for all analyses. We did not adjust P values but focused on ankle-joint sagittal- and frontal-plane angles and moments as primary variables due to the preliminary nature of our study.[23]

RESULTS

Participants

Participants had 4.2 ± 3.3 total ankle sprains, 4.5 ± 6.3 episodes of giving way within the 6 months before the study, an IdFAI score of 23.5 ± 4.5, a FAAM–Activities of Daily Living score of 82.8% ± 6.7%, and a FAAM-Sports score of 66.8% ± 10.2%. The mean and SDs for the captured data are presented in Table 1. All associations among JCF and independent variables with r values of $\geq$0.3 are

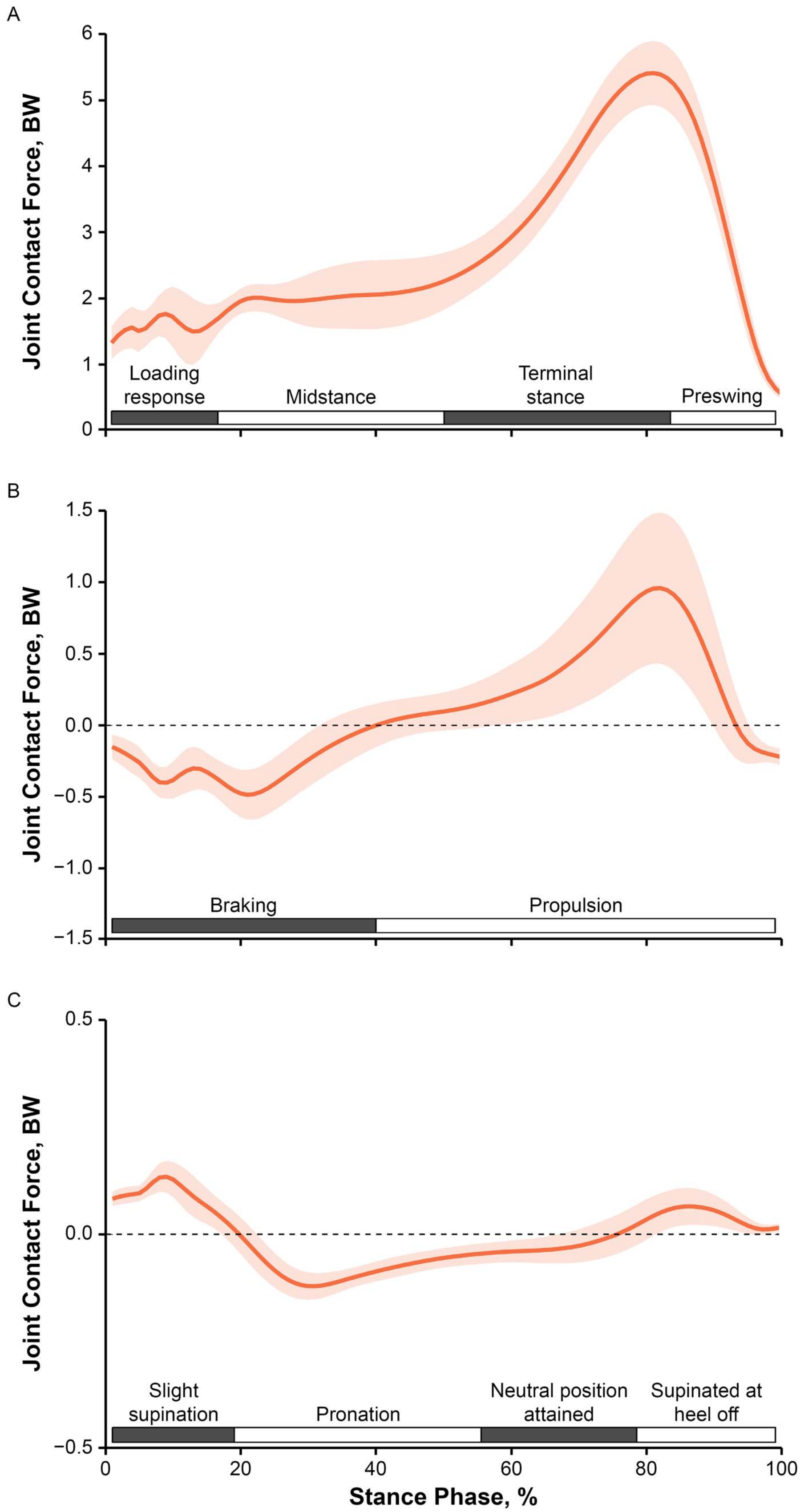

Figure 2. Triaxial ankle-joint contact force during stance phases of walking. Joint contact force < 0 indicates posterior and medial directions, as shown in B and C, respectively. A, Compressive joint contact force. B, Anteroposterior shear joint contact force. C, Mediolateral shear joint contact force. Abbreviation: BW, body weight.

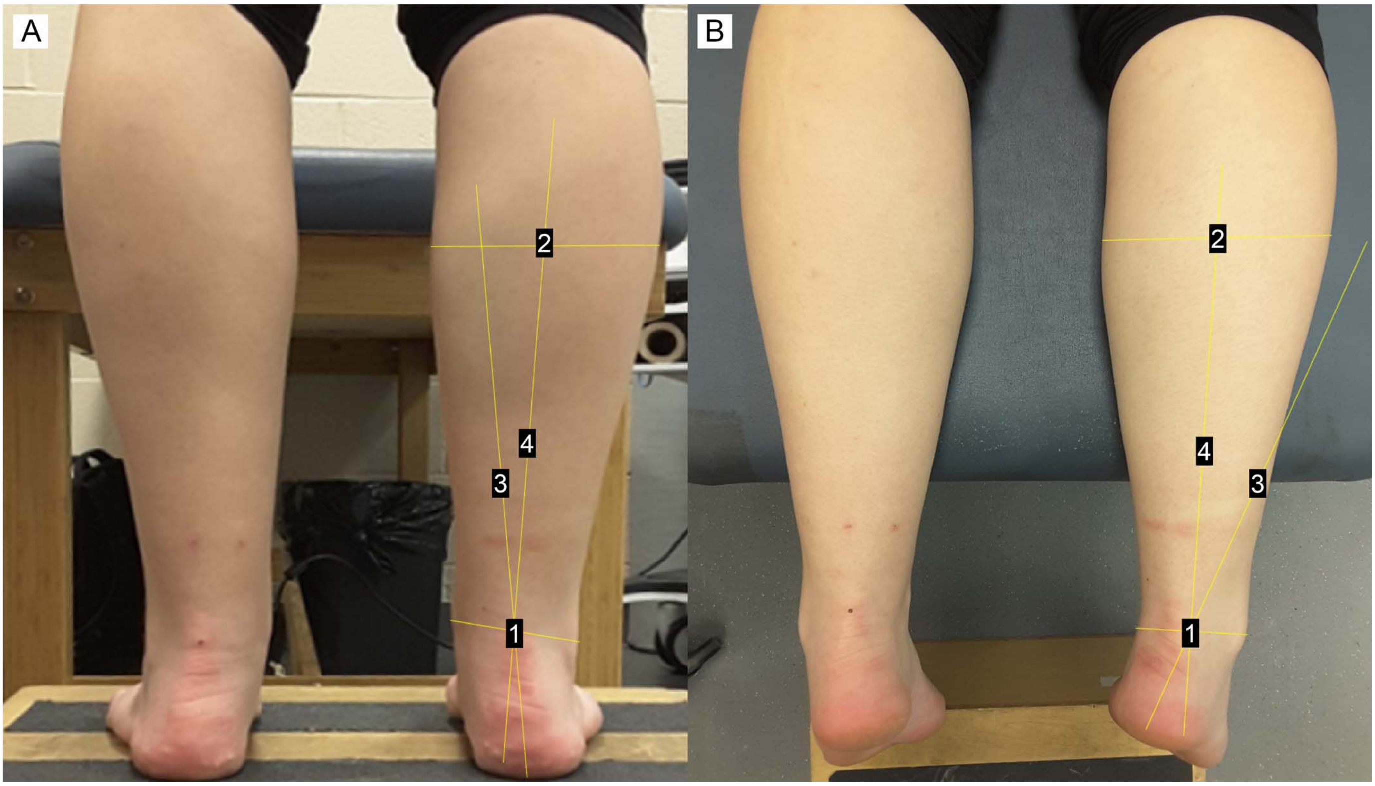

Figure 3. Rearfoot varus alignment measurements. A, Weight-bearing position. B, Non–weight-bearing position. 1, Midpoint between the lateral and medial malleoli; 2, midpoint of the widest part of the calf, used to bisect the leg; 3, line extending from the center of the heel (posterior view) to the midpoint between the malleoli, representing the calcaneal bisecting line; and 4, line connecting the midpoint of the widest part of the calf to the midpoint between the malleoli, representing the leg bisecting line.

reported in Table 2. The results of the multivariable regressions are presented in Table 3.

Compressive Ankle JCF

More WB rearfoot varus alignment (Figure 4A) was associated with lower compressive JCF peak and interpreted as a large association ($r = -0.53$, $P = .02$). Both WB rearfoot alignment and peak inversion moment were included in the multivariable linear regression model and together explained 40.4% of the compressive JCF peak variance ($R^2 = 0.404$, $F_{3,17} = 3.842$, $P = .03$). A greater compressive JCF impulse was associated with smaller peak plantar-flexion angle, with the correlation interpreted as large ($r = 0.51$, $P = .02$;) (Figure 5A), and greater peak dorsiflexion moment, with the correlation interpreted as moderate ($r = 0.46$, $P = .042$) (Figure 5B). Both peak plantar-flexion angle and moment were included in the regression model and together explained 50.2% of the compressive JCF impulse variance ($R^2 = 0.502$, $F_{3,17} = 5.709$, $P = .007$). Greater compressive JCF LR was associated with a greater peak inversion moment, with the correlation interpreted as moderate ($r = -0.46$, $P = .041$; Figure 6). Peak inversion moment, peak plantar-flexion moment, and SEBT-PM were included in the regression analysis and explained 34.2% of the compressive JCF LR variance ($R^2 = 0.350$, $F_{4,16} = 2.151$, $P = .058$).

Posterior Shear Ankle JCF

Greater posterior shear JCF peak was associated with greater peak eversion ($r = 0.55$, $P = .01$), dorsiflexion ($r = -0.48$, $P = .03$), inversion ($r = -0.46$, $P = .04$), and plantar-flexion ($r = 0.45$, $P = .044$) moments (Figure 7). More NWB rearfoot varus alignment was associated with a lower posterior shear JCF peak ($r = 0.51$, $P = .02$; Figure 7B). These correlations were interpreted as moderate to large. Peak eversion, inversion, dorsiflexion, and plantar-flexion moments; peak rearfoot alignment; and peak plantar-flexion angle were included in the regression model and together explained 66.9% of the posterior shear JCF peak variance ($R^2 = 0.669$, $F_{7,13} = 3.758$, $P = .02$). A more NWB rearfoot varus alignment (Figure 8) was associated with lower posterior shear JCF LR ($r = 0.47$, $P = .04$), interpreted as a moderate effect. Non–weight-bearing rearfoot alignment and peak dorsiflexion moment were included in the regression analysis and explained 42.6% of the variance in posterior shear JCF LR ($R^2 = 0.426$, $F_{3,17} = 4.214$, $P = .048$).

Lateral Shear Ankle JCF

Greater peak dorsiflexion moment was associated with greater lateral shear JCF peak, and the association was interpreted as moderate ($r = 0.49$, $P = .03$; Figure 9). Peak dorsiflexion moment and NWB rearfoot alignment were included in the regression analysis and explained 45.6% of the lateral shear JCF peak variance ($R^2 = 0.456$, $F_{3,17} = 4.749$, $P = .03$). More NWB rearfoot varus alignment was also associated with lower lateral shear JCF impulse, and the association was interpreted as large ($r = -0.52$, $P = .02$; Figure 10A). Greater lateral shear JCF impulse was associated with greater peak dorsiflexion moment ($r = 0.49$, $P = .03$) and peak inversion angle ($r = 0.47$, $P = .04$), and the association was interpreted as moderate (Figure 10). Non–weight-bearing

Table 1. Descriptive Statistics for Regression Variables for CAI (N = 21)

Variable	Mean ± SD
Joint contact force	
Compressive	
Peak, BW	5.55 ± 0.53
Impulse, BW·s	1.92 ± 0.22
Loading rate, BW/s	8.43 ± 1.58
Anteroposterior shear	
First peak, BW	−0.67 ± 0.18
First impulse, BW·s	−0.08 ± 0.02
First loading rate, BW/s	−5.80 ± 2.40
Second peak, BW	1.02 ± 0.53
Second impulse, BW·s	0.15 ± 0.11
Second loading rate, BW/s	3.69 ± 1.10
Mediolateral shear	
First peak, BW	0.17 ± 0.05
First impulse, BW·s	0.01 ± 0.00
First loading rate, BW/s	1.92 ± 0.78
Second peak, BW	−0.13 ± 0.03
Second impulse, BW·s	−0.03 ± 0.01
Second loading rate, BW/s	−2.10 ± 0.54
Third peak, BW	0.08 ± 0.04
Third impulse, BW·s	0.01 ± 0.01
Third loading rate, BW/s	0.54 ± 0.14
Structural and functional	
Weight-bearing lunge test, cm	9.69 ± 3.56
Star Excursion Balance Test	
Anterior	0.66 ± 0.06
Posteromedial	0.72 ± 0.11
Posterolateral	0.81 ± 0.09
Rearfoot alignment,°	
Weight-bearing	5.44 ± 2.98
Non–weight-bearing	10.90 ± 8.55
Gait biomechanics	
Peak dorsiflexion angle,°	12.0 ± 5.30
Peak plantar-flexion angle,°	−7.18 ± 3.36
Peak dorsiflexion moment, Nm/kg	0.52 ± 0.18
Peak plantar-flexion moment, Nm/kg	−1.59 ± 0.48
Peak inversion angle,°	17.8 ± 4.60
Peak eversion angle,°	6.27 ± 4.39
Peak eversion moment, N·m/kg	−0.06 ± 0.07
Peak inversion moment, N·m/kg	0.27 ± 0.10

Abbreviations: BW, body weight; CAI, chronic ankle instability.

Table 2. Pearson Partial Correlations Between Triaxial Ankle Joint Contact Force Outcome and Traditional Biomechanics, Rearfoot Alignment, Dynamic Postural Control, and Patient-Reported Outcome Variables, After Accounting for Gait Speed

Joint Contact Force Variable	Variable	r Value	P Value[a]
Compressive			
Peak	Weight-bearing rearfoot alignment	−0.53	.02[b]
	Peak inversion moment	−0.38	.10
Impulse	Peak plantar-flexion angle	0.51	.02[b]
	Peak dorsiflexion moment	0.46	.042[b]
Loading rate	Peak inversion moment	−0.46	.041[b]
	Peak plantar-flexion moment	0.43	.058
	Star Excursion Balance Test—posteromedial	0.37	.10
Posterior			
Peak	Peak eversion moment	0.55	.01[b]
	Non–weight-bearing rearfoot alignment	0.51	.02[b]
	Peak dorsiflexion moment	−0.48	.03[b]
	Peak inversion moment	−0.46	.04[b]
	Peak plantar-flexion moment	0.45	.044[b]
	Peak plantar-flexion angle	0.40	.08
Loading rate	Non–weight-bearing rearfoot alignment	0.47	.04[b]
	Peak dorsiflexion moment	−0.43	.06
Lateral			
Peak	Peak dorsiflexion moment	0.49	.03[b]
	Non–weight-bearing rearfoot alignment	−0.43	.06
Impulse	Non–weight-bearing rearfoot alignment	−0.52	.02[b]
	Peak dorsiflexion moment	0.49	.03[b]
	Peak inversion angle	0.47	.04[b]
	Peak eversion moment	−0.43	.06
	Peak plantar-flexion moment	−0.40	.08

[a] Variables with $P < .10$ were included to explore trend toward significance.
[b] Indicates difference ($P < .05$).

rearfoot alignment, peak dorsiflexion moment, peak inversion angle, peak eversion moment, and peak plantar-flexion moment were included in the regression analysis and explained 47.4% of the lateral shear JCF impulse variance ($R^2 = 0.475$, $F_{6,14} = 2.111$, $P = .057$).

DISCUSSION

Our goal was to explore associations between ankle JCF and other CAI-related impairments. The results indicated that triaxial ankle JCF during walking in patients with CAI is associated with structural measures, postural control, and walking biomechanics, consistent with our hypotheses. However, the directions of several biomechanical and structural associations were contrary to our hypotheses. Cumulatively, our findings suggested that multiple impairments are associated with ankle JCF in those with CAI.

Compressive Ankle JCF

Consistent with our hypothesis, greater rearfoot alignment (ie, varus position) during WB was associated with lower compressive ankle JCF peak. Patients with CAI exhibit lower compressive ankle JCF during pushing off the ground in walking and landing relative to uninjured individuals.[11,24] Excessive rearfoot varus is one of the mechanical alterations often found in those with CAI. This compromised foot position is known to increase susceptibility to repetitive ankle sprains at heel contact by causing the foot to adopt a more supinated position, which may accelerate the degenerative process over time. Patients with CAI exhibit increased lateral foot pressure while pushing off the ground during walking compared with uninjured controls.[25] This increased lateral foot pressure contributes to a greater ankle-inversion moment.[25,26] Although this remains speculative, greater rearfoot varus may further contribute to an increased inversion moment as the foot progresses into the toe-off phase during walking, potentially exacerbating the risk of injury and degeneration process. Thus, our findings suggest that greater rearfoot varus alignment in patients with CAI is linked to altered ankle-loading patterns during gait, warranting further attention to elucidate if mechanical joint loading contributes to the early onset of ankle-joint degeneration in patients with CAI.

Greater peak plantar-flexion angle and less dorsiflexion moment were found to be associated with a reduced compressive ankle JCF impulse. The JCF impulse is used to quantify the total mechanical loading on the ankle throughout the stance phase of walking by calculating the area under the force-time curve. Notably, greater peak plantar-flexion angle and less peak dorsiflexion moment, particularly occurring

Table 3. Hierarchical Multivariable Regression Analysis for Triaxial Ankle-Joint Contact Force Outcomes Under Traditional Biomechanics, Rearfoot Alignment, and Dynamic Postural Control

Joint Contact Force Variable	Variable[a]	1	2	3	4	5	6	7
Compressive								
Peak	Gait speed	0.993	1.213	0.902	b	b	b	b
	Weight-bearing rearfoot alignment		−0.091[c]	−0.082[c]	b	b	b	b
	Peak inversion moment			−1.540	b	b	b	b
	Constant	4.209[d]	4.409[d]	5.191[d]	b	b	b	b
	R^2	0.071	0.327	0.404	b	b	b	b
	ΔR^2		0.256	0.077	b	b	b	b
Impulse	Gait speed	−0.637[e]	−0.789[c]	−1.035[d]	b	b	b	b
	Peak plantar-flexion angle		0.031[c]	0.027[c]	b	b	b	b
	Peak dorsiflexion moment			0.464[e]	b	b	b	b
	Constant	2.779[d]	3.201[d]	3.267[d]	b	b	b	b
	R^2	0.173	0.387	0.502	b	b	b	b
	ΔR^2		0.214	0.115	b	b	b	b
Loading rate	Gait speed	0.082	−1.314	−1.296	−1.004	b	b	b
	Peak inversion moment	b	−7.464[c]	−5.046	−1.711	b	b	b
	Peak plantar-flexion moment	b	b	0.704	1.281	b	b	b
	Star Excursion Balance Test—posteromedial	b	b	b	5.242	b	b	b
	Constant	8.317[c]	12.205[d]	12.648[d]	8.514[e]	b	b	b
	R^2	0	0.212	0.233	0.350	b	b	b
	ΔR^2	b	0.211	0.021	0.117	b	b	b
Posterior								
Peak	Gait speed	−0.406[d]	−0.260	−0.156	−0.048	−0.180	−0.072	−0.041
	Peak eversion moment	b	1.406[c]	1.197[c]	1.072[c]	0.679	0.879	0.345
	Non–weight-bearing rearfoot alignment	b	b	0.008[c]	0.007[e]	0.008[e]	0.007	0.007[e]
	Peak dorsiflexion moment	b	b	b	−0.251	−0.196	−0.318	−0.554[e]
	Peak inversion moment	b	b	b	b	0.409	0.554	0.303
	Peak plantar-flexion moment	b	b	b	b	b	−0.087	−0.111
	Peak plantar-flexion angle	b	b	b	b	b	b	0.023
	Constant	−0.119	−0.234	−0.477	−0.483	−0.259	−0.422	−0.314
	R^2	0.107	0.379	0.527	0.570	0.596	0.608	0.669
	ΔR^2	b	0.272	0.148	0.043	0.026	0.012	0.061
Loading rate	Gait speed	−7.182[e]	−3.815	−3.435	b	b	b	b
	Peak dorsiflexion moment	b	−5.809[e]	−4.046	b	b	b	b
	Non–weight-bearing rearfoot alignment	b	b	0.094	b	b	b	b
	Constant	3.907	2.361	−0.088	b	b	b	b
	R^2	0.182	0.336	0.426	b	b	b	b
	ΔR^2	b	0.154	0.090	b	b	b	b
Lateral								
First peak	Gait speed	0.164[c]	0.086	0.080	b	b	b	b
	Peak dorsiflexion moment	b	0.134[c]	0.105[e]	b	b	b	b
	Non–weight-bearing rearfoot alignment	b	b	−0.002	b	b	b	b
	Constant	−0.052	−0.016	0.024	b	b	b	b
	R^2	0.214	0.400	0.456	b	b	b	b
	ΔR^2		0.186	0.056	b	b	b	b
First impulse	Gait speed	0.003	0.001	−0.002	−0.001	−0.002	−0.002	b
	Non–weight-bearing rearfoot alignment	b	−0.0002[c]	−0.0001[e]	−0.0001	−0.0001	−0.0001	b
	Peak dorsiflexion moment	b	b	0.005	0.005	0.004	0.004	b
	Peak inversion angle	b	b	b	0.0001	0.0001	0.0001	b
	Peak eversion moment	b	b	b		−0.011	−0.012	b
	Peak plantar-flexion moment	b	b	b	b	b	0.0002	b
	Constant	0.007	0.012[c]	0.012[c]	0.010	0.010	0.011	b
	R^2	0.029	0.287	0.386	0.400	0.475	0.475	b
	ΔR^2	b	0.258	0.099	0.014	0.075	0	b

[a] Gait speed was included as the initial predictor block for each model because ankle kinematics and kinetics are influenced by gait speed.
[b] Indicates that the variable was not included in the respective regression model.
[c] Indicates difference ($P < .05$).
[d] Indicates difference ($P < .01$).
[e] Indicates $P < .10$. Variable included to explore trend toward significance.

during the initial contact phase, could lead to a diminished compressive ankle JCF impulse. Thus, concluding that this reduction occurs mainly by decreasing the area under the curve, especially during the heel-strike phase, seems reasonable. In individuals with CAI, the ankle JCF impulse during walking and landing have been reported to be lower compared with that in uninjured individuals.[11,24] Although the implications of lower compressive ankle JCF on cartilage health remain

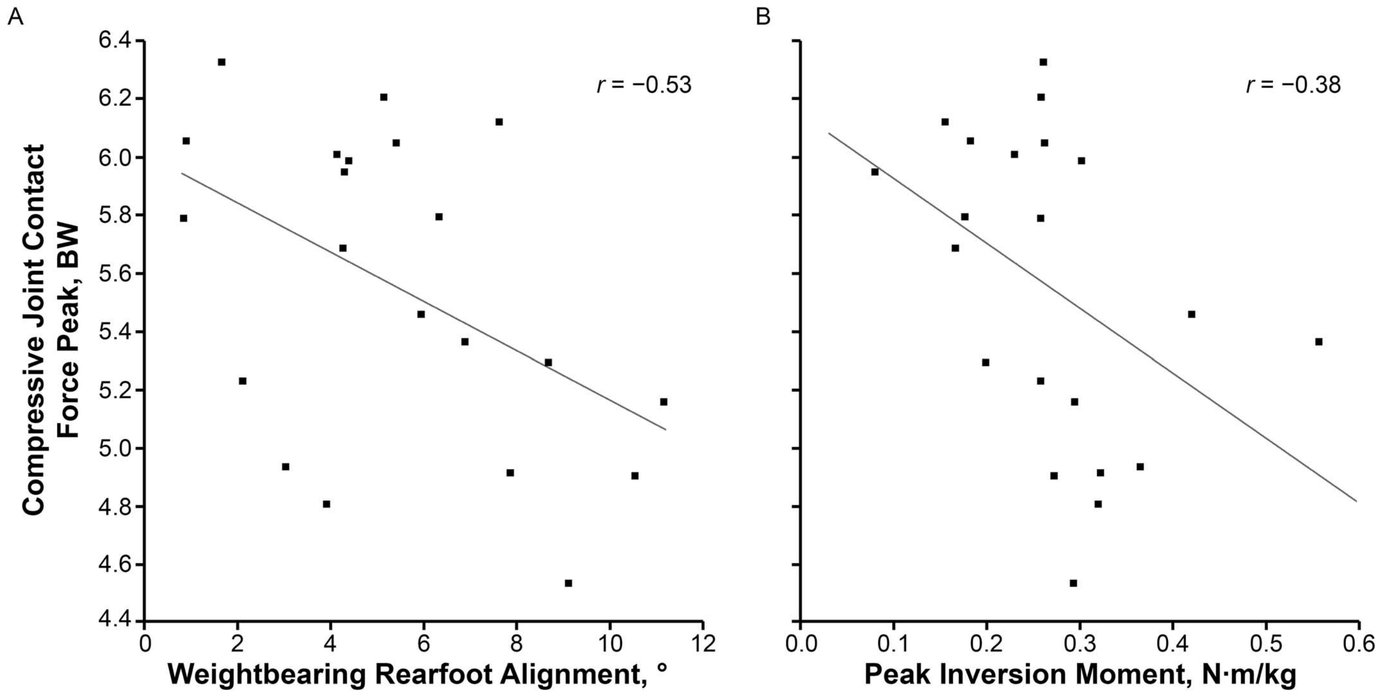

Figure 4. Scatterplots between compressive joint contact force peak and A, weight-bearing rearfoot alignment, and B, peak inversion moment. Abbreviation: BW, body weight.

unknown, several speculations exist. First, lower compressive ankle JCF is thought to result largely from weakened triceps surae muscle strength, as muscle force is the primary contributor to JCF.[9] Researchers have observed that patients with CAI have diminished muscle volume in the triceps surae.[27] Reduced muscle size, function, or both are thought to be a strong indicator of progressive joint degeneration.[28] Second, a notable link exists between CAI and degenerative posttraumatic ankle osteoarthritis, with both conditions exhibiting similarly reduced muscle volume in the triceps surae compared with uninjured controls.[28,29] Third, similar patterns of reduced JCF at the tibiofemoral joint have been observed in patients after anterior cruciate ligament reconstruction, partly due to diminished muscle force, which is thought to contribute to the deterioration of tibiofemoral cartilage health and accelerate early joint degeneration.[4,30]

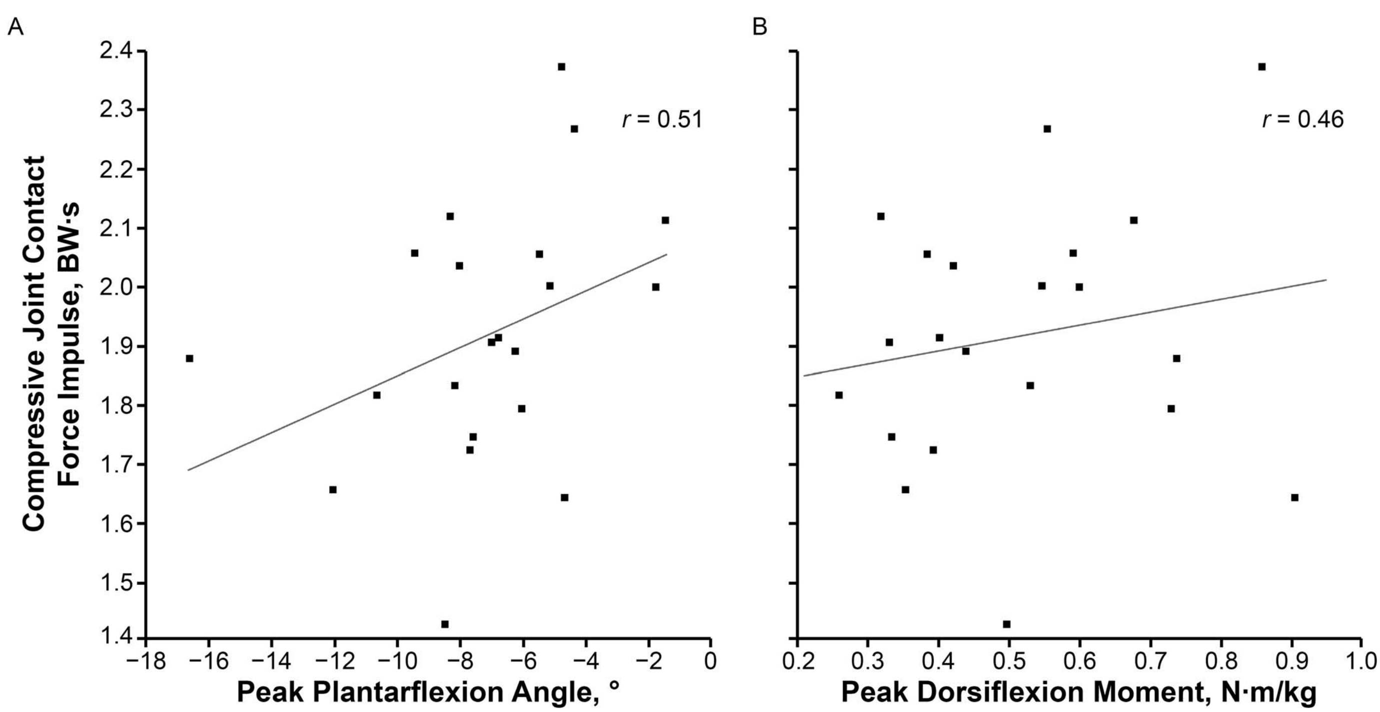

Figure 5. Scatterplots between compressive joint contact force impulse and A, peak plantar-flexion angle, and B, peak dorsiflexion moment. Abbreviation: BW, body weight.

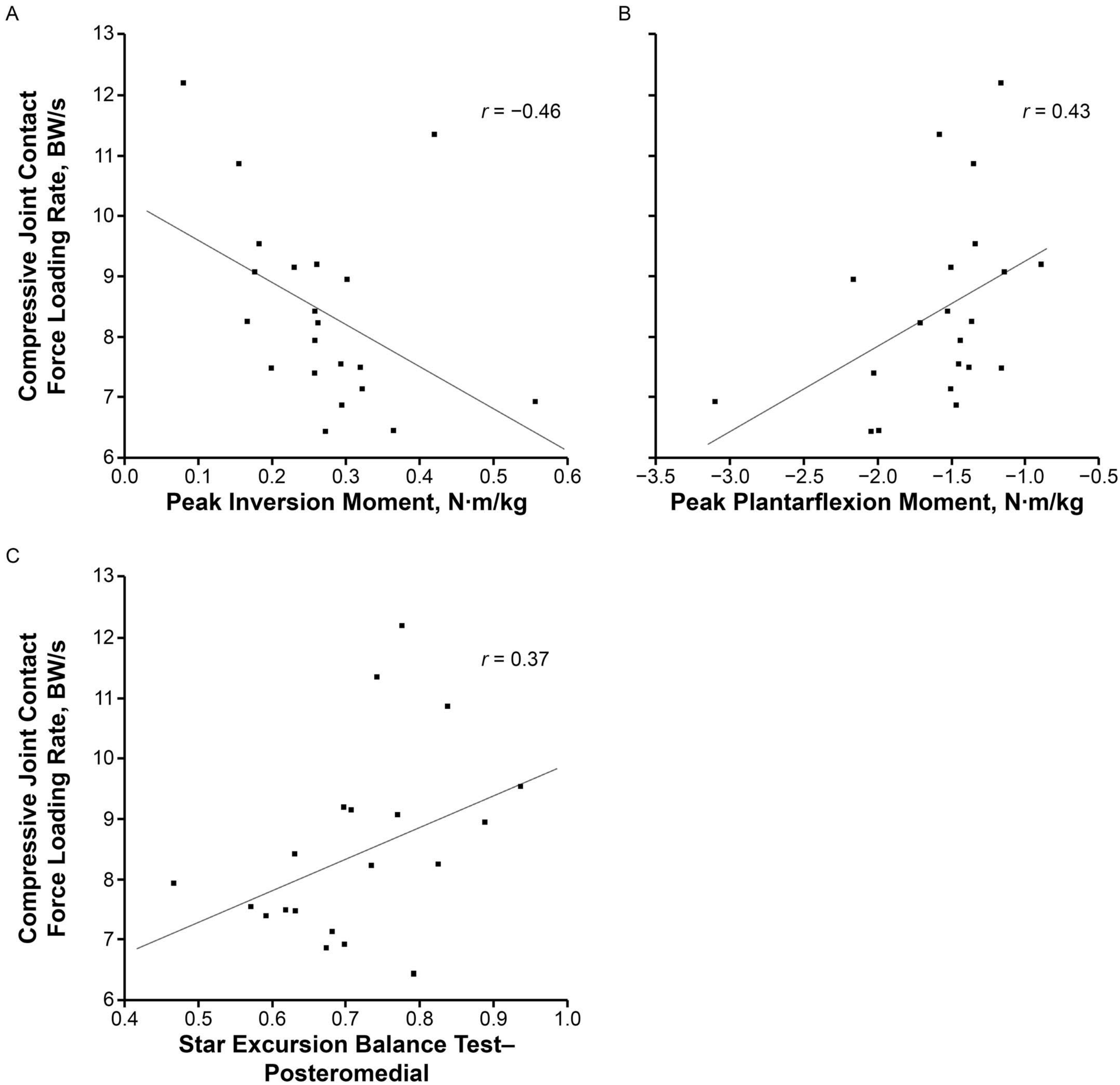

Figure 6. Scatterplots between compressive joint contact force loading rate and A, peak inversion moment, B, peak plantar-flexion moment, and C, Star Excursion Balance Test—posteromedial direction. Abbreviation: BW, body weight.

However, the above-mentioned speculation, although based on existing data, has not been proven. Prospective studies should be conducted to validate these hypotheses and further explore the relationship between joint mechanics and the progression of degenerative conditions in patients with CAI.

Posterolateral Shear JCF

Peak Eversion and Dorsiflexion Moment. Our findings indicated that greater posterolateral JCF is associated with greater peak eversion and dorsiflexion moment, occurring primarily at heel strike. Individuals with CAI demonstrate elevated posterolateral shear JCF during the heel-strike phase of walking compared with uninjured controls.[11] Furthermore, those with CAI have increased activation of the peroneus longus from preswing to heel strike, a compensatory mechanism aimed at everting a foot that has become more inverted during the preswing phase.[31–33] This is presumably followed by a large eversion moment right after heel strike. Despite some controversy, increased tibialis anterior activation has also been observed in individuals with CAI during heel strike and helps stabilize the foot through dorsiflexion.[26,34] This action not only generates a dorsiflexion moment but also leads to an inversion moment, potentially exacerbating a laterally deviated foot position after heel strike. This altered foot positioning heightens the risk of recurrent ankle sprains and may elucidate the link between greater posterolateral ankle JCF and the peak inversion angle and moment observed during

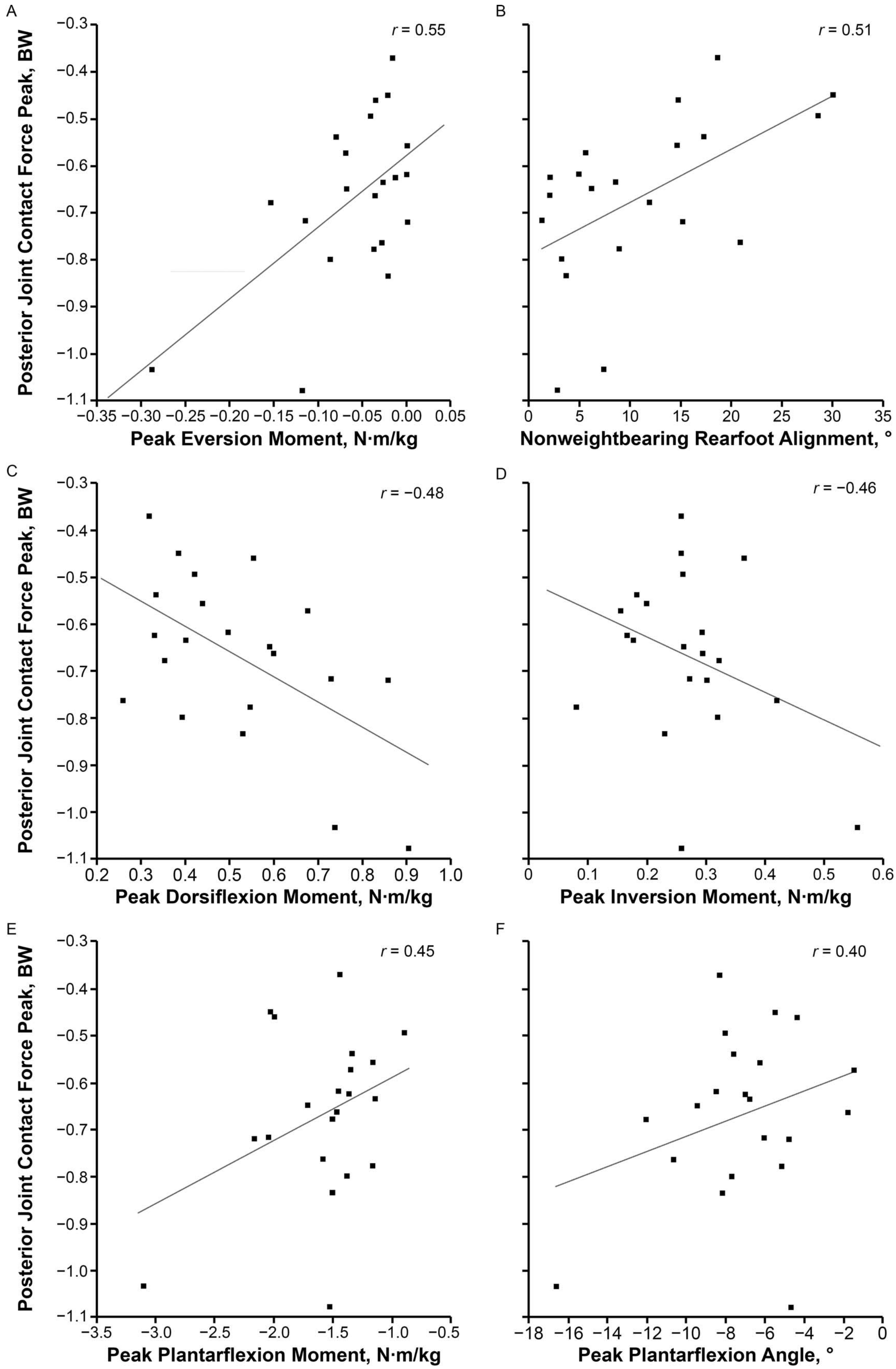

Figure 7. Scatterplots between posterior joint contact force peak and, A, peak eversion moment, B, non–weight-bearing rearfoot alignment, C, peak dorsiflexion moment, D, peak inversion moment, E, peak plantar-flexion moment, and F, peak plantar-flexion angle. Abbreviation: BW, body weight.

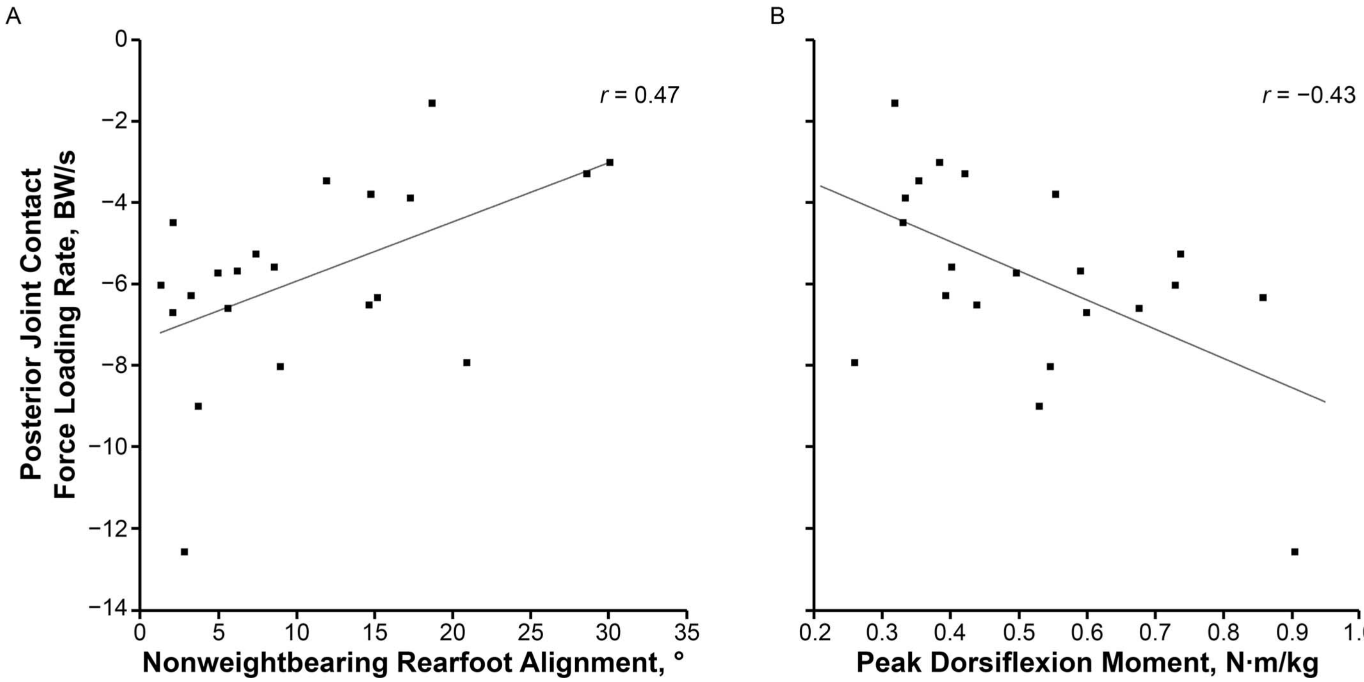

Figure 8. Scatterplots between posterior joint contact force loading rate and A, non–weight-bearing rearfoot alignment, and B, peak dorsiflexion moment. Abbreviation: BW, body weight.

the push-off phase. Assuming our goal is to make their elevated posterolateral JCF comparable to that of uninjured individuals, our treatment objective could be to reduce posterolateral ankle JCF via therapeutic intervention. Given that JCF is a factor amenable to nonoperative intervention, addressing it using tailored rehabilitation strategies could offer a promising avenue for reducing the recurrence of ankle sprains and improving stability in those with CAI.[35] Specifically, AP joint mobilization of the talus or mobilization with a movement technique (ie, Mulligan technique) could be beneficial to address altered posterolateral ankle JCF.

Rearfoot Varus. Contrary to our hypothesis, patients with CAI showed consistent associations between greater rearfoot varus during NWB and lower lateral JCF during heel strike (ie, first peak and first impulse). Interestingly, we also identified the same pattern of associations between less compressive and posterior shear JCF and greater rearfoot varus. Patients with CAI are known to walk with less stride-to-stride variability

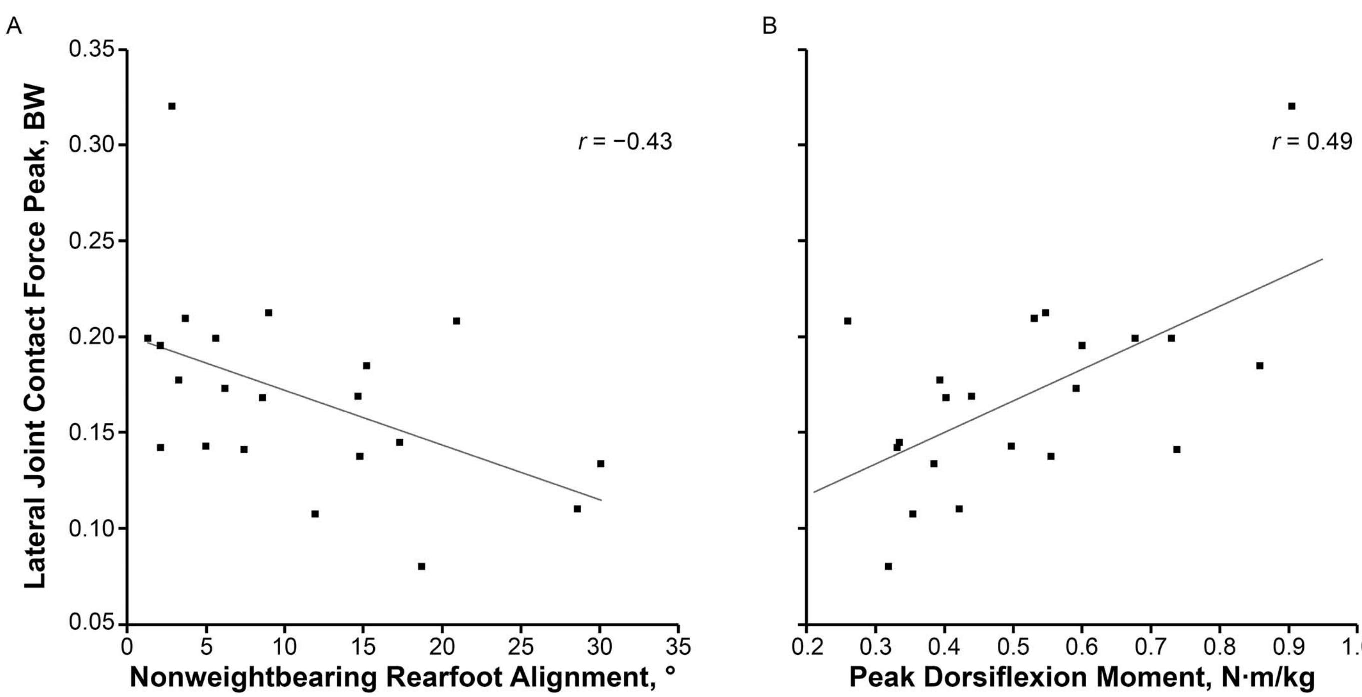

Figure 9. Scatterplots between lateral joint contact force peak and A, non–weight-bearing rearfoot alignment, and B, peak dorsiflexion moment. Abbreviation: BW, body weight.

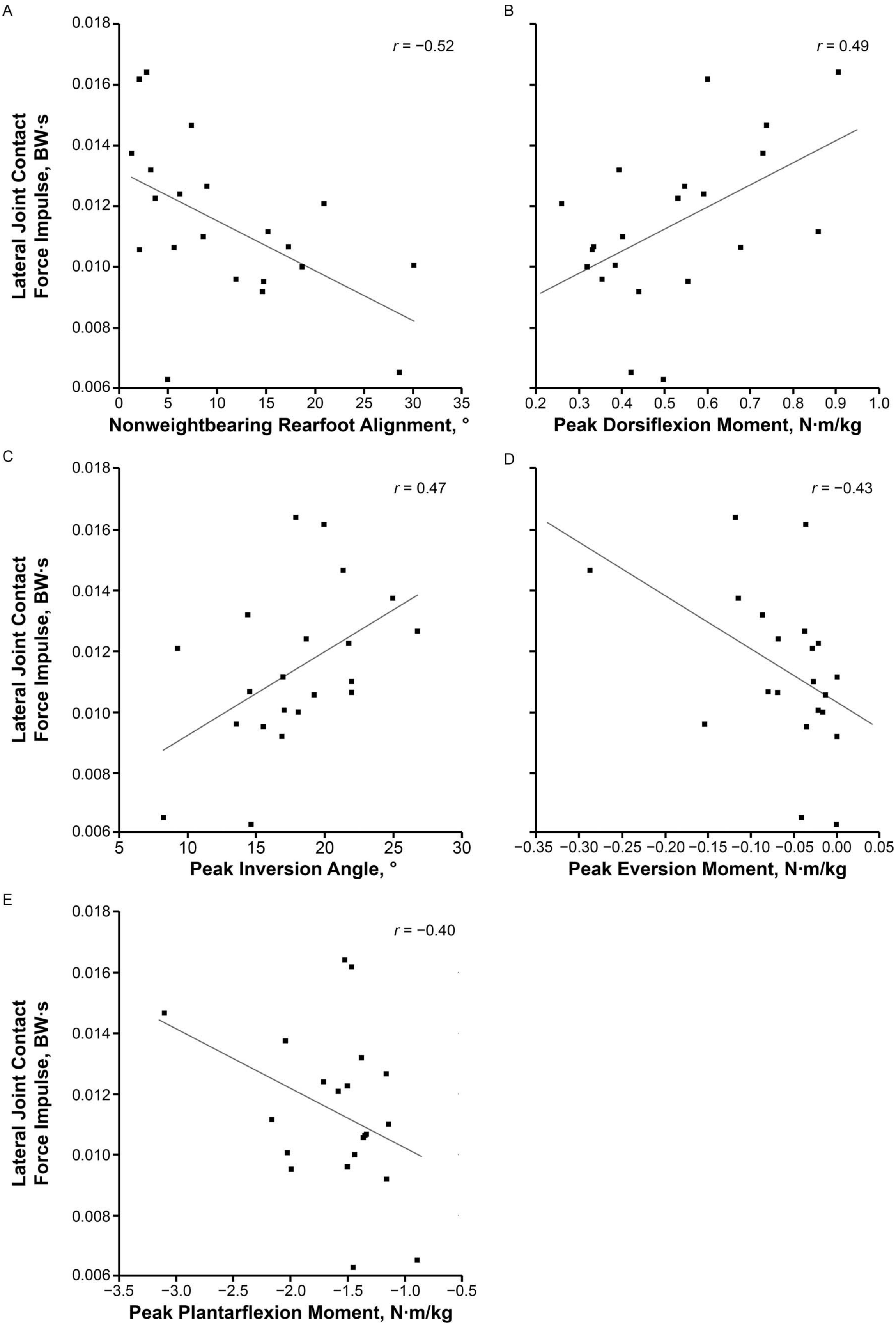

Figure 10. Scatterplots between lateral joint contact force impulse and A, non–weight-bearing rearfoot alignment, B, peak dorsiflexion moment, C, peak inversion angle, D, peak eversion moment, and E, peak plantar-flexion moment. Abbreviation: BW, body weight.

of shank-rearfoot joint coupling, indicating more constrained and less adaptable ankle kinematics.[36] Koldenhoven et al suggested that this rigid kinematics pattern is attributed to a more laterally deviated center of pressure, as it could limit the normal degrees of freedom available as well as the ability to respond to subtle alterations.[37] Cumulatively, our results combined with previous findings suggest that greater rearfoot varus could lead to more rigid ankle kinematics and lower triaxial JCF throughout the stance phase of walking. Although a more laterally deviated foot position is modifiable via gait retraining with specific types of feedback in patients with CAI, interventions to address reduced stride-to-stride variability have yet to be investigated. Based on the results of our regression models for posterior JCF peak and LR and lateral JCF peak and impulse, peak dorsiflexion and eversion moment as well as rearfoot alignment could be used to predict ankle JCF in patients with CAI.

Limitations

This study had limitations. First, due to the cross-sectional design, we do not know if the identified modifiable variables that were associated with triaxial ankle JCF were the root cause of JCF or a downstream effect of JCF alterations. Second, using the widest point of the calf to calculate a rearfoot alignment does not reflect the exact alignment of the tibia. Although this method was based on previous research, a better way to define the *lower leg line* in future investigations would be to use radiography or computed tomography to visualize bony structures.[19,20] Third, a small sample size was included in this preliminary study. The identified associations suggest that structural and postural control outcomes and gait biomechanics could be therapeutic targets to slow disease progression, but future prospective studies are needed to validate our findings. However, we analyzed a larger study sample than most modeling investigations to address this limitation, if not completely, then at least partially. Fourth, we also do not know if the identified variables associated with ankle JCF are exclusively in patients with CAI or if such associations would also be present in uninjured controls. Fifth, we could not validate our calculated ankle JCF values, as no such data are available. However, we followed standardized procedures from the OpenSim manual to estimate JCF. We also do not know whether altered ankle-joint loading in individuals with CAI directly causes the early onset of ankle-joint degeneration. Sixth, only indirect validation of our model (Rajagopal et al) exists for kinematic and kinetic outcomes.[14] However, our study is still meaningful because the model's accuracy is supported by comparisons of muscle excitation and measured muscle activation in the original validation study. For example, if earlier steps (eg, scaling and inverse kinematics) were incorrect, further calculations such as muscle excitation estimation would also be wrong, as subsequent steps rely on previous results. Lastly, when a traditional inverse dynamics approach is used to quantify frontal-plane ankle-joint kinetics, some uncertainty can arise regarding the precise position of the center of pressure when using a force-instrumented treadmill. This may lead to variability in signal-to-noise ratios. Despite this, our approach followed widely accepted methods used in the field, contributing valuable insights to the understanding of ankle-joint mechanics.

CONCLUSIONS

Based on the observed associations, improving peak moments or strength (all 4 directions), WB and NWB rearfoot alignment, dynamic postural control (SEBT-PM), and range of motion could be used to predict ankle JCF in patients with CAI during walking. Our results are meaningful and contribute to the understanding of CAI-related biomechanics, provided that we interpret them within the context of the complex interplay between joint moments, muscle forces, and JCF. This approach does not limit our interpretation but rather enriches it by acknowledging the comprehensive framework within which musculoskeletal modeling operates.

ACKNOWLEDGMENTS

This study was supported by grant 1516OGP001 from the National Athletic Trainers' Association Research and Education Foundation (Dr Wikstrom).

REFERENCES

1. Waterman BR, Owens BD, Davey S, Zacchilli MA. The epidemiology of ankle sprains in the United States. *J Bone Joint Surg Am*. 2010;92(13):2279–2284. doi:10.2106/JBJS.I.01537
2. Anandacoomarasamy A, Barnsley L. Long term outcomes of inversion ankle injuries. *Br J Sports Med*. 2005;39(3):e14. doi:10.1136/bjsm.2004.011676
3. Hertel J, Corbett RO. An updated model of chronic ankle instability. *J Athl Train*. 2019;54(6):572–588. doi:10.4085/1062-6050-344-18
4. Wellsandt E, Gardinier ES, Manal K, Axe MJ, Buchanan TS, Snyder-Mackler L. Decreased knee joint loading associated with early knee osteoarthritis after anterior cruciate ligament injury. *Am J Sports Med*. 2016;44(1):143–151. doi:10.1177/0363546515608475
5. Delco ML, Kennedy JG, Bonassar LJ, Fortier LA. Post-traumatic osteoarthritis of the ankle: a distinct clinical entity requiring new research approaches. *J Orthop Res*. 2017;35(3):440–453. doi:10.1002/jor.23462
6. Anderson DD, Chubinskaya S, Guilak F, et al. Post-traumatic osteoarthritis: improved understanding and opportunities for early intervention. *J Orthop Res*. 2011;29(6):802–809. doi:10.1002/jor.21359
7. Wikstrom EA, Song K, Tennant JN, Pietrosimone B. Gait biomechanics and balance associate with talar and subtalar T1ρ relaxation times in those with chronic ankle instability. *Med Sci Sports Exerc*. 2022;54(6):1013–1019. doi:10.1249/MSS.0000000000002867
8. Wikstrom EA, Song K, Casey M, et al. T1rho MRI of the subtalar articular cartilage is increased in those with chronic ankle instability. *Osteoarthritis Cartilage*. 2019;27(suppl 1):S316–S317.
9. Prinold JA, Mazzà C, Di Marco R, et al; MD-PAEDIGREE Consortium. A patient-specific foot model for the estimate of ankle joint forces in patients with juvenile idiopathic arthritis. *Ann Biomed Eng*. 2016;44(1):247–257. doi:10.1007/s10439-015-1451-z
10. Seth A, Hicks JL, Uchida TK, et al. OpenSim: simulating musculoskeletal dynamics and neuromuscular control to study human and animal movement. *PLoS Comput Biol*. 2018;14(7):e1006223. doi:10.1371/journal.pcbi.1006223
11. Jang J, Wikstrom EA. Ankle joint contact force profiles differ between those with and without chronic ankle instability during walking. *Gait Posture*. 2023;100:1–7. doi:10.1016/j.gaitpost.2022.11.012
12. Gabriner ML, Houston MN, Kirby JL, Hoch MC. Contributing factors to Star Excursion Balance Test performance in individuals with chronic ankle instability. *Gait Posture*. 2015;41(4):912–916. doi:10.1016/j.gaitpost.2015.03.013
13. Gribble PA, Delahunt E, Bleakley C, et al. Selection criteria for patients with chronic ankle instability in controlled research: a position statement

of the International Ankle Consortium. *Br J Sports Med*. 2014;48(13): 1014–1018. doi:10.1136/bjsports-2013-093175
14. Rajagopal A, Dembia CL, DeMers MS, Delp DD, Hicks JL, Delp SL. Full-body musculoskeletal model for muscle-driven simulation of human gait. *IEEE Trans Biomed Eng*. 2016;63(10):2068–2079. doi:10.1109/tbme.2016.2586891
15. Kim H, Palmieri-Smith R, Kipp K. Muscle force contributions to ankle joint contact forces during an unanticipated cutting task in people with chronic ankle instability. *J Biomech*. 2021;124:110566. doi:10.1016/j.jbiomech.2021.110566
16. Sturdy JT, Silverman AK, Pickle NT. Automated optimization of residual reduction algorithm parameters in OpenSim. *J Biomech*. 2022;137:111087. doi:10.1016/j.jbiomech.2022.111087
17. Zargham A, Afschrift M, De Schutter J, Jonkers I, De Groote F. Inverse dynamic estimates of muscle recruitment and joint contact forces are more realistic when minimizing muscle activity rather than metabolic energy or contact forces. *Gait Posture*. 2019;74:223–230. doi:10.1016/j.gaitpost.2019.08.019
18. Miller RH, Krupenevich RL, Pruziner AL, Wolf EJ, Schnall BL. Medial knee joint contact force in the intact limb during walking in recently ambulatory service members with unilateral limb loss: a cross-sectional study. *PeerJ*. 2017;5:e2960. doi:10.7717/peerj.2960
19. Gross KD, Niu J, Zhang YQ, et al. Varus foot alignment and hip conditions in older adults. *Arthritis Rheum*. 2007;56(9):2993–2998. doi:10.1002/art.22850
20. Matsuda S, Fukubayashi T, Hirose N. Characteristics of the foot static alignment and the plantar pressure associated with fifth metatarsal stress fracture history in male soccer players: a case-control study. *Sports Med Open*. 2017;3(1):27. doi:10.1186/s40798-017-0095-y
21. Bennell KL, Talbot RC, Wajswelner H, Techovanich W, Kelly DH, Hall AJ. Intra-rater and inter-rater reliability of a weight-bearing lunge measure of ankle dorsiflexion. *Aust J Physiother*. 1998;44(3):175–180. doi:10.1016/s0004-9514(14)60377-9
22. Plante JE, Wikstrom EA. Differences in clinician-oriented outcomes among controls, copers, and chronic ankle instability groups. *Phys Ther Sport*. 2013;14(4):221–226. doi:10.1016/j.ptsp.2012.09.005
23. Feise RJ. Do multiple outcome measures require p-value adjustment? *BMC Med Res Methodol*. 2002;2:8. doi:10.1186/1471-2288-2-8
24. Jang J, Franz JR, Pietrosimone BG, Wikstrom EA. Muscle contributions to reduced ankle joint contact force during drop vertical jumps in patients with chronic ankle instability. *J Biomech*. 2024;163:111926. doi:10.1016/j.jbiomech.2024.111926
25. Son SJ, Kim H, Seeley MK, Hopkins JT. Altered walking neuromechanics in patients with chronic ankle instability. *J Athl Train*. 2019;54(6): 684–697. doi:10.4085/1062-6050-478-17
26. Hopkins JT, Coglianese M, Glasgow P, Reese S, Seeley MK. Alterations in evertor/invertor muscle activation and center of pressure trajectory in participants with functional ankle instability. *J Electromyogr Kinesiol*. 2012;22(2):280–285. doi:10.1016/j.jelekin.2011.11.012
27. Feger MA, Snell S, Handsfield GG, et al. Diminished foot and ankle muscle volumes in young adults with chronic ankle instability. *Orthop J Sports Med*. 2016;4(6):2325967116653719. doi:10.1177/2325967116653719
28. Wiewiorski M, Dopke K, Steiger C, Valderrabano V. Muscular atrophy of the lower leg in unilateral post traumatic osteoarthritis of the ankle joint. *Int Orthop*. 2012;36(10):2079–2085. doi:10.1007/s00264-012-1594-6
29. Valderrabano V, von Tscharner V, Nigg BM, et al. Lower leg muscle atrophy in ankle osteoarthritis. *J Orthop Res*. 2006;24(12):2159–2169. doi:10.1002/jor.20261
30. Saxby DJ, Bryant AL, Modenese L, et al. Tibiofemoral contact forces in the anterior cruciate ligament-reconstructed knee. *Med Sci Sports Exerc*. 2016;48(11):2195–2206. doi:10.1249/mss.0000000000001021
31. Moisan G, Mainville C, Descarreaux M, Cantin V. Kinematic, kinetic and electromyographic differences between young adults with and without chronic ankle instability during walking. *J Electromyogr Kinesiol*. 2020;51:102399. doi:10.1016/j.jelekin.2020.102399
32. Feger MA, Donovan L, Hart JM, Hertel J. Lower extremity muscle activation in patients with or without chronic ankle instability during walking. *J Athl Train*. 2015;50(4):350–357. doi:10.4085/1062-6050-50.2.06
33. Delahunt E, Monaghan K, Caulfield B. Altered neuromuscular control and ankle joint kinematics during walking in subjects with functional instability of the ankle joint. *Am J Sports Med*. 2006;34(12):1970–1976. doi:10.1177/0363546506290989
34. Louwerens JW, van Linge B, de Klerk LW, Mulder PG, Snijders CJ. Peroneus longus and tibialis anterior muscle activity in the stance phase: a quantified electromyographic study of 10 controls and 25 patients with chronic ankle instability. *Acta Orthop Scand*. 1995;66(6):517–523. doi:10.3109/17453679509002306
35. Jang J, Migel KG, Kim H, Wikstrom EA. Acute vibration feedback during gait reduces mechanical ankle joint loading in chronic ankle instability patients. *Gait Posture*. 2021;90:261–266. doi:10.1016/j.gaitpost.2021.09.171
36. Herb CC, Chinn L, Dicharry J, McKeon PO, Hart JM, Hertel J. Shank-rearfoot joint coupling with chronic ankle instability. *J Appl Biomech*. 2014;30(3):366–372. doi:10.1123/jab.2013-0085
37. Koldenhoven RM, Feger MA, Fraser JJ, Saliba S, Hertel J. Surface electromyography and plantar pressure during walking in young adults with chronic ankle instability. *Knee Surg Sports Traumatol Arthrosc*. 2016;24(4):1060–1070. doi:10.1007/s00167-016-4015-3

Address correspondence to Jaeho Jang, PhD, ATC, Department of Kinesiology, 1851 Wiggins Rd, Rm 452, El Paso, TX 79968. Address email to jjang2@utep.edu.